Brain Microstructure assessed by CHARMED and NODDI in the newborn

Nicolas Kunz[1], Hui Zhang[2], Yaniv Assaf[3], François Lazeyras[4], Daniel Alexander[2], and Petra Susan Hüppi[1,5]

[1]*Pediatrics, University of Geneva, Geneva, Switzerland,* [2]*Computer Science, University College London, London, United Kingdom,* [3]*Neurobiology, Tel Aviv University, Tel Aviv, Israel,* [4]*Radiology-CIBM, Geneva University Hospitals, Geneva, Switzerland,* [5]*Department of Neurology, Children's Hospital, Geneva, Switzerland*

PURPOSE This work investigates the microstructural basis of standard diffusion tensor imaging (DTI) measures during early brain development. The last trimester of pregnancy and the first months of life are two critical periods of brain development, as disruptions during these periods are known to lead to many neurobiological disorders and cognitive disabilities. Diffusion weighted (DW) MRI is presently the only feasible technique for non-invasively studying the tissue microstructural changes occurring during this time. DTI, the standard DW-MRI model, has shown great sensitivity to microstructural changes by providing indices such as fractional anisotropy (FA) and mean diffusivity (MD) [1]. However, these parameters do not have the specificity to assess specific developmental changes separately, such as ongoing myelination or changes in axonal density and geometry. To enable the assessment of such specific changes, a number of multi-compartment models have been recently developed. The two models of particular interest are the composite hindered and restricted model of diffusion (CHARMED) [2], which models white matter (WM) in terms of two (intra- and extra-axonal) compartments, and the neurite orientation dispersion and density imaging (NODDI) model [3], which models both gray and white matter. They require only modest increase in imaging time, hence are attractive for imaging brain development. Here, we use DW imaging data appropriate for fitting multi-compartment models to understand the relationship between the standard DTI-derived indices and the estimates from CHARMED and NODDI in neonates for the first time.

METHODS Subjects: 6 newborns born between 29 and 40 weeks of gestation were scanned at term (40^{th} of gestational age) in accordance to local ethical committee. Imaging: All imaging was conducted on a 3T Siemens Trio system. The data were acquired using a double refocusing spin echo echo-planar imaging pulse sequence. Acquisition parameters were: TE/TR = 95/3500ms, spatial resolution 2×2×2mm^3, matrix = 80×80, and 22 axial slices centered on the corpus callosum. Diffusion imaging scheme: 66 DW images with 3 reference b_0 images. The remaining 63 non-collinear directions were split into 5 shells with b-values ranging from 50 to 2500 s/mm^2. The acquisition time was 4 mins. Image Processing: **1.** Diffusion tensor (DT) images for each subjects were reconstructed with Camino [4] using only the 4 first shells (i.e. bmax = 1400 s/mm^2, 56 directions); **2.** DT images were then spatially normalized to the study-specific DT template using DTI-TK [5]; **3.** The regions of interest (ROI) are drawn on the study-specific template; **4.** ROIs are transformed back to the subject space to compute ROI-averaged estimates from DTI, CHARMED, and NODDI maps. **1.A.** The CHARMED and NODDI models are also estimated using Camino, with intra-axonal diffusivity (D_{ic}) fixed to 2x10^{-3} mm^2/s and isotropic diffusivity to 3x10^{-3} mm^2/s. A tortuosity model was used for the perpendicular extra-cellular diffusivity ($D_{ec,\perp}=(1-\nu_{ic})\cdot D_{ic}$), which correspond to a simplified version of the original CHARMED model. The estimated CHARMED parameters are intra-cellular volume fraction (ν_{ic}) and isotropic volume fraction (ν_{iso}); the estimated NODDI parameters additionally include orientation dispersion index (ODI). Signal was modeled as: $S/S_0=(1-\nu_{iso})\cdot[\nu_{ic}\cdot S_{ic}+(1-\nu_{ic})\cdot S_{ec}]+\nu_{iso}\cdot S_{iso}$ **2.A** We additionally warp the CHARMED and NODDI parameter maps to the template space to generate corresponding group averages.

RESULTS & DISCUSSION DT Template: The scalar maps of the DT template (Fig. 1) allow easy identification of the newborn WM tracts and for ROIs definition (Fig. 2). Indeed, low FA fibers, e.g. external capsule (eCaps) and posterior/anterior thalamic radiation (p/a-tr), were barely visible on single subject maps, but they can be clearly identified in the template. ROI drawing on a template has the additional advantage of minimizing the inter-subject variation but requires a high quality spatial alignment between the subjects and the template. Our choice of DTI-TK ensures this, as it employs tensor-based registration that aligns WM more accurately than alternative tools [6]. DTI: Results were in good agreement with literature [1]. The highest FA values are found in the corpus callosum regions: splenium (CC-sp), body (CC-bd), and genu (CC-ge). Mean diffusivity (MD) and FA distinguish the different stages of myelination of the anterior and posterior limbs of the internal capsule (iCaps-a with no myelin and iCaps-p myelinated, respectively). The other WM regions show similar values to the iCaps-a (Table 1). CHARMED and NODDI: As DTI, both new methods were able to differentiate the different stages of myelination of the iCaps-p and iCaps-a with lower ν_{ic} values for the latter, where no myelin is present. The intra-cellular volume fraction ν_{ic} estimated from CHARMED shows a similar trend as FA: the highest values in CC and much lower values for iCaps-p and the other tracts. By estimating both ν_{ic} and ODI, NODDI appears to provide an even finer separation of different microstructural contributors to FA. In contrast to CHARMED, which reports lower values of ν_{ic} for iCaps-p than for CC, NODDI finds similar values of ν_{ic} for both tracts. It differentiates the two tracts by orientation dispersion, with iCaps-p having much lower ODI value than CC. This is consistent with CC being the most densely-packed and organized tract in the entire brain, which explains its high FA despite the lack of myelin, whereas the higher dispersion in iCaps-p leads to its lower FA than CC, despite the presence of myelin. Their similar ν_{ic} can be due to the fact that the high packing density in CC compensates for its lack of myelin and the presence of myelin in iCaps-p compensates for its lower packing density. In addition, iCaps-a has lower ν_{ic} than iCaps-p, consistent with their difference in myelination. The lower ODI in iCaps-p than in iCaps-a is similarly plausible, because it is reasonable to expect that the myelinated fibers are packed more tightly than the non-myelinated ones and fanning of fibers in the posterior limb is less pronounced than in the anterior limb of the internal capsule. Finally, ODI gives a new important measure of areas presenting fiber crossing or large fanning, including the iCaps-a, external capsule (eCaps), centrum semiovale (cso) and the periventricular area (pva).

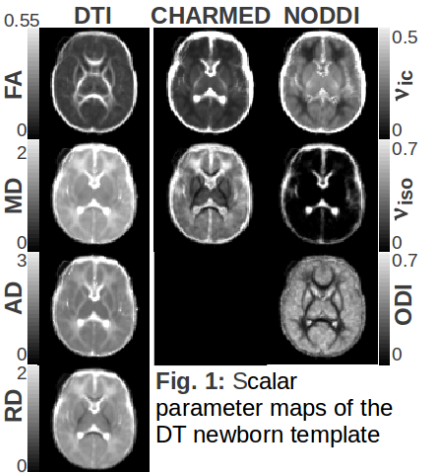

Fig. 1: Scalar parameter maps of the DT newborn template

CONCLUSION We demonstrate for the first time the use of multi-compartment models to separate the microstructural factors contributing to the DTI findings in newborn, which are apart from fiber density, degree of myelination and fiber geometry like fanning or dispersion. Given the small sample size, these results are preliminary and future work will include additional subjects at different gestational and maturational age

REFERENCES [1] Hüppi, PedR98, [2] Assaf,MRM04 [3] Zhang,NIMG12 [4] Cook,ISMRM06 [5] Zhang MedIA06 [6] Wang,NIMG12. **Acknowledgements** Supported by the CIBM of the UNIL, UNIGE, HUG, CHUV, EPFL, Leenards and Jeantet foundation, the SNSF (32-102127) and CONNECT EU FP7.

Table 1: ROIs Mean ± std values in newborn scanned at term at 3T. Diffusivity (mean, MD; axial, AD=λ_1; and radial, RD=$(\lambda_2+\lambda_3)/2$) are given in 10^{-3} mm^2/s.

	DTI				CHARMED		NODDI		
	FA	MD	AD	RD	ν_{ic}	ν_{iso}	ν_{ic}	ν_{iso}	ODI
CC-sp	0.66 ± 0.05	1.24 ± 0.07	2.35 ± 0.04	0.69 ± 0.11	0.34 ± 0.03	0.17 ± 0.07	0.35 ± 0.04	0.08 ± 0.02	0.03 ± 0.00
CC-bd	0.48 ± 0.03	1.48 ± 0.11	2.33 ± 0.09	1.05 ± 0.12	0.29 ± 0.04	0.23 ± 0.09	0.29 ± 0.02	0.17 ± 0.06	0.08 ± 0.02
CC-ge	0.55 ± 0.03	1.45 ± 0.12	2.49 ± 0.33	0.92 ± 0.05	0.27 ± 0.04	0.18 ± 0.04	0.28 ± 0.04	0.12 ± 0.05	0.06 ± 0.03
iCaps-p	0.46 ± 0.02	1.08 ± 0.02	1.68 ± 0.01	0.77 ± 0.02	0.23 ± 0.01	0.00 ± 0.00	0.33 ± 0.01	0.00 ± 0.00	0.15 ± 0.00
iCaps-a	0.30 ± 0.02	1.20 ± 0.04	1.62 ± 0.07	0.99 ± 0.03	0.16 ± 0.01	0.00 ± 0.00	0.25 ± 0.02	0.00 ± 0.00	0.23 ± 0.05
eCaps	0.24 ± 0.02	1.24 ± 0.03	1.55 ± 0.04	1.09 ± 0.04	0.13 ± 0.01	0.00 ± 0.00	0.22 ± 0.01	0.00 ± 0.00	0.27 ± 0.02
pva	0.18 ± 0.01	1.51 ± 0.09	1.79 ± 0.11	1.37 ± 0.09	0.09 ± 0.01	0.09 ± 0.06	0.13 ± 0.03	0.00 ± 0.00	0.24 ± 0.04
cso	0.27 ± 0.02	1.35 ± 0.06	1.70 ± 0.05	1.17 ± 0.07	0.11 ± 0.01	0.00 ± 0.01	0.19 ± 0.02	0.00 ± 0.00	0.22 ± 0.02

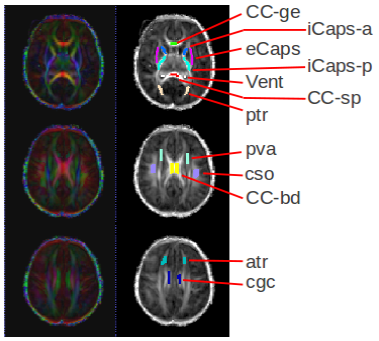

Fig 2: RGB and FA newborn templates with ROI's overlaid